Superconducting Filter for IMT-2000 Band

Genichi Tsuzuki, *Member, IEEE*, Masanobu Suzuki, and Nobuyoshi Sakakibara

***Abstract*—In this paper, a new design of microstrip-line superconducting filters for IMT-2000 band application is presented. The design features high selectivity by means of creating transmission zeros and using many resonators. As a demonstration, a 16- and 32-pole filter were fabricated using YBCO films on a half-area and on the full area of 3-in-diameter MgO wafers, respectively. Excellent attenuation of more than 30 dB, 420 kHz from the lower band edge, and 400 kHz from the upper band edge for the 32-pole filter was achieved. The filters were tuned not with mechanical tuning screws, but with a dielectric film. The tuning was carried out based on a novel method of measurement. These techniques are also described.**

***Index Terms*—Cross-coupling, filter, superconductor, tuning.**

I. Introduction

WE PREVIOUSLY presented a superconducting filter for the IMT-2000 band, having a 5-MHz bandwidth [1]. The filter featured the narrow bandwidth because superconducting filters are advantageous over conventional filters for narrow-bandwidth applications due to their high unloaded-Q factor. The filter consisted of ring resonators that were arranged in a circle. The ring resonator filter realized both narrow bandwidth and compact size through the form of the resonator and the arrangement. As the next goal, we present basestation receiver filters for the IMT-2000 band, having a 20-MHz bandwidth and a 1930-MHz center frequency. We focused on a 20-MHz bandwidth because it is considered as the widest bandwidth of a channel in the IMT-2000 system. Furthermore, it is more difficult to obtain a steep skirt slope for a 20-MHz bandwidth than for a narrower bandwidth, such as 5 MHz, because the degree of the skirt slope decreases in proportion to bandwidth. RF filters are required to have steep skirt responses to cut off signals of neighboring channels or of other systems. If the RF filters cannot sufficiently cut off such out-band signals, a low-noise amplifier and/or other nonlinear devices may cause distortion signals of higher order intermodulation into its own channel by the out-band signals. The distortion signals will badly affect communication quality, which will be a major problem for the IMT-2000 system.

Prompted by the above situation, we developed two kinds of filters. One features both a steep skirt cutoff response and excellent low insertion loss achieved by using 16 resonators. The other features outstanding even steeper skirt cutoff performance through the use of 32 resonators. These filters were designed following the idea of the resonator's arrangement of the ring resonator filter, but by improving the shape of the ring resonator. In this paper, a J-shaped hairpin resonator was proposed to create transmission zeros at both band edges and to pack more resonators into the limited wafer area. By introducing J-shaped hairpin resonators and the circular arrangement, the filter could accommodate 16 resonators on a half-area or 32 resonators on a full area of a 3-in-diameter wafer and exhibited excellent steep skirt cutoff performance.

Filter tuning is also presented. The tuning process is carried out by a novel method of measurement of design parameters of a filter such as resonant frequency. A dielectric thin film was deposited on each resonator to shift its resonant frequency based on the information obtained from the measurement. As a result of this permanent tuning, the filters need no mechanical tuning screws.

Manuscript received March 1, 2000; revised August 23, 2000.
The authors are with Cryodevice Inc., Aichi 470-0111, Japan.
Publisher Item Identifier S 0018-9480(00)10783-5.

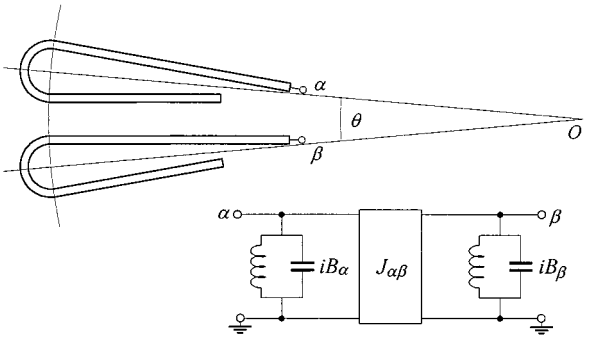

Fig. 1. Layout of coupling J-shaped hairpin resonators and its equivalent circuit.

II. Filter Design

A. J-Shaped Hairpin Resonator

A cross-coupling technique to create transmission zeros has been developed [2], [3] for the realization of steep skirt band-edge slope. The technique has also been applied to several lumped-element planar high-temperature superconductor (HTS) filters [4], [5]. In those studies, transmission zeros were created at the desired frequencies by intentionally introducing cross couplings into the circuit and adjusting them. However, it is not so easy to control only the intentional cross couplings using the distributed element planar configuration because unwanted cross couplings are unavoidable in the configuration. In other words, coupling itself between distant resonators is intrinsic in the propagation of electromagnetic energy in this configuration.

We take another approach to realize transmission zeros for distributed element filters. By this approach, transmission zeros will appear at both band edges through the effect of all cross couplings, not by only some intentional cross couplings. We propose a J-shaped hairpin resonator and an arrangement of the resonators. Fig. 1 shows the configuration of the J-shaped hairpin resonator and the arrangement. The J-shaped resonator

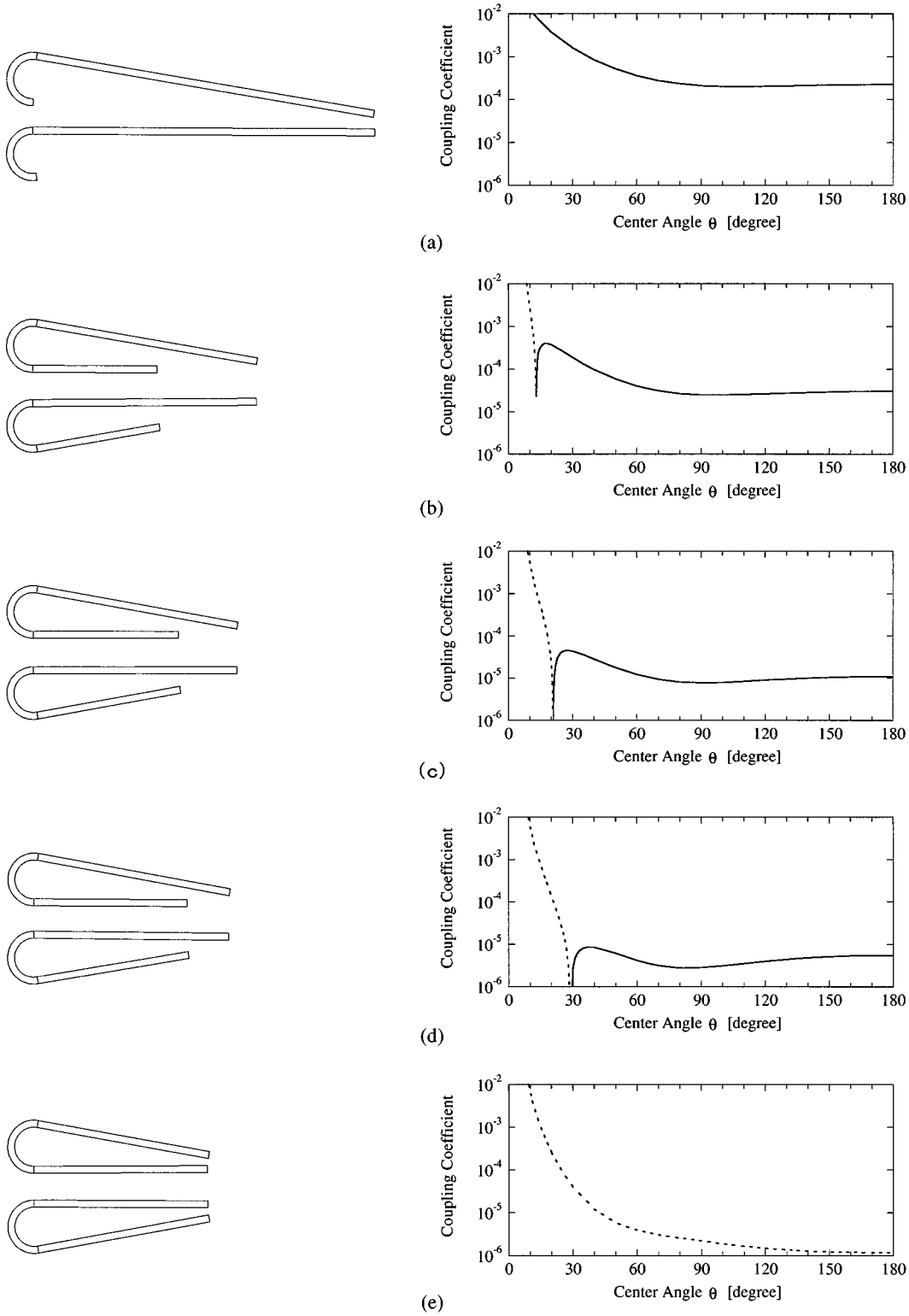

Fig. 2. Several kinds of J-shaped resonator's forms and their coupling coefficients' dependence on center angle. Solid line denotes positive sign and dashed line denotes negative sign of coupling.

consists of an arc and two lines. Each resonator is arranged on a circle to accommodate as many resonators as possible in a limited wafer area. Coupling intensity between J-shaped resonators is controlled by adjusting the center angle θ between them and the ratio of two lines' length of the resonator.

The coupling coefficient $k_{\alpha\beta}$ between two ports α and β in an equivalent circuit in Fig. 1 is defined and given as [6]

$$k_{\alpha\beta} = \frac{J_{\alpha\beta}}{\sqrt{b_\alpha b_\beta}}$$

where $J_{\alpha\beta}$ is the admittance inverter parameter and b_i is the resonator slope parameter at the resonant frequency f_0 defined as

$$b_L = \frac{f_0}{Z} - \left.\frac{\partial B_L}{\partial f}\right|_{f=f_0}, \qquad i = \alpha, \beta.$$

The resonator susceptance jB_i and the admittance inverter parameter $J_{\alpha\beta}$ are related to the Y-matrix elements between ports α and β as

$$iB_\alpha = Y_{\alpha\alpha} \quad iB_\beta = Y_{\beta\beta} \quad J_{\alpha\beta} = |Y_{\alpha\beta}|.$$

The coupling coefficient's dependence on the center angle was examined for several configurations illustrated in Fig. 2. The coefficient was calculated at 1930 MHz, which was the center frequency of the filters presented in this paper, using a commercial two-dimensional (2-D) electromagnetic (EM) simulator. The ratio of the lengths of two lines differs in Fig. 2(a)–(e). The configuration in Fig. 2(a) has a positive sign of coupling independent of its center angle, while the configuration in Fig. 2(e) has a negative sign independent of its center angle. In the cases of configurations from Fig. 2(b)–(d), each coupling changes its sign at the center angle. This indicates that both the sign and magnitude of coupling are controllable by adjusting the ratio of the two line's lengths of the J-shaped resonator. In this paper, we adopted the configuration in Fig. 2(c) to realize filters having a steep skirt cutoff response in a limited wafer area.

B. J-Shaped Hairpin Resonator Filters

Two kinds of Chebyshev response filters were designed as examples of the J-shaped hairpin resonator filters. They consisted of 16 resonators and 32 resonators. The design specifications were a 1.09% bandwidth and a 0.02-dB passband ripple for the 16-pole filter, and a 1.06% bandwidth and a 0.005-dB passband ripple for the 32-pole filter. The bandwidth for the 16-pole filter was designed to be slightly wider than that for the 32-pole filter because the design of the 16-pole filter was aimed at achieving not only a steep skirt, but also low insertion loss and low group delay deviation by expanding the bandwidth.

As shown in Fig. 2(c), the coupling changes its sign from negative to positive at the point $\theta = 20.8$ degree. With this change of the sign, transmission zeros appear at both band edges for the two filters, making the skirt slope steeper. Fig. 3 shows simulated results for the two filters. The results were calculated using an equivalent-circuit model. The model consisted of resonators, couplings between terminal resonators and input/output load, couplings between adjacent resonators and cross couplings between nonadjacent resonators. All cross coupling paths were taken into account for the 16-pole filter. For the 32-pole filter, cross coupling paths shorter than 16 intervals of resonators were considered. For example, coupling between the first resonator and the seventeenth resonator was taken into account, but coupling between the first resonator and the eighteenth resonator was not. Couplings between farther resonators farther apart than 17 intervals were ignored because the EM shield described in the following section obstructed them. The simulation predicted that transmission zeros would appear at both band edges. Such transmission zeros would be the results of the change of the sign of coupling mentioned above.

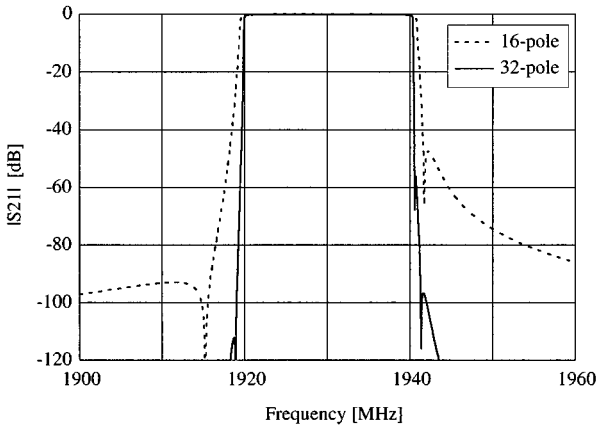

Fig. 3. Simulated results for the 16-pole filter plotted by dashed line and for the 32-pole filter plotted by solid line.

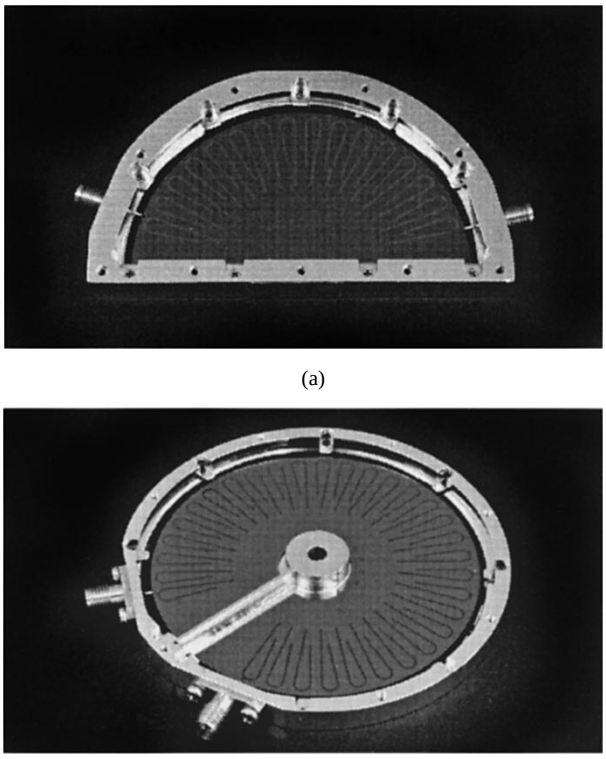

(a)

(b)

Fig. 4. (a) 16-pole filter. (b) 32-pole filter.

III. Fabrication and Measurement

The 16- and 32-pole filters were fabricated using YBCO films on a half-area and on the full area of 3-in-diameter MgO wafers, respectively. Fig. 4 shows their photographs. For the 32-pole filter, a keyhole shape was cut out of the wafer, in which to set an EM shield in the filter case, as shown in Fig. 4(b), using a YAG laser cutting machine. The shield, which consists of a column and partition, obstructed unwanted shortcut cross coupling among far resonators, in particular, direct coupling between input and output resonators. This idea was carried over from our previous paper [1].

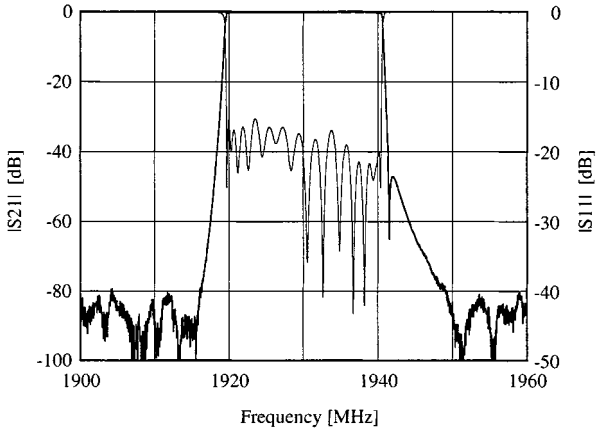

Fig. 5. Measured responses at 70 K for: (a) the 16- and (b) the 32-pole filters.

Fig. 5 shows measured responses for the two filters at 70 K. In both results, a transmission zero appeared at the upper band edge. The result agreed with the prediction of the simulation results shown in Fig. 3. A transmission zero at the lower band edge for both filters and another one at the upper band edge for the 32-pole filter, which were predicted by the simulation, could not be distinguished because of the influence of the background noise of around -90 dB. However, the measured responses showed consistent agreement with the simulation results regarding the bandwidth and skirt slope.

Table I shows the performance of the two filters. The 16-pole filter achieved an excellent insertion loss of less than 0.4 dB, while it attenuated out-band signals of 30 dB, 1280 kHz from the lower band edge, and 1150 kHz from the higher band edge. The return loss was better than 15 dB and group delay deviation was about 300 ns. The 32-pole filter exhibited outstanding selectivity performance. The filter attenuated out-band signals of 30 dB, 420 kHz from the lower band edge, and 400 kHz from the higher band edge. The filter also exhibited a good insertion loss of less than 1.2 dB in spite of a lot of pole numbers. This result was achieved due to the high unloaded-Q factor of the resonators of around 120 000 at 70 K.

Fig. 6 shows the measurement of distortion of third-order intermodulation (IM3) at 70 K for the 16-pole filter. The input intercept point of IM3 at 1930 MHz caused by two in-band fundamental signals, which were 1933 and 1936 MHz, was as high as

TABLE I
PERFORMANCE OF 16- AND 32-POLE FILTERS AT 70 K

ITEMS		16-pole	32-pole
Insertion Loss	1920 MHz	0.36 dB	1.15 dB
	Minimum	0.14 dB	0.32 dB
	1940 MHz	0.25 dB	1.08 dB
Skirt Steepness (30dB attenuation)	Lower Side	1918.72 MHz	1919.58 MHz
	Upper Side	1941.15 MHz	1940.40 MHz
Return Loss		15 dB<	15 dB<
Group Delay Deviation		300 nsec	1500 nsec

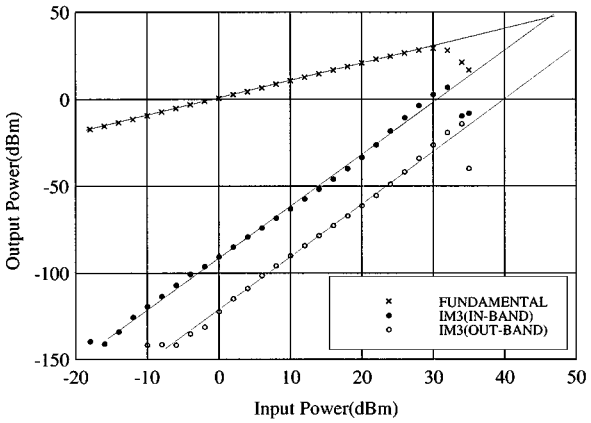

Fig. 6. Measurement of IM3 for the 16-pole filter at 70 K. The solid circle denotes IM3 at 1930 MHz caused by in-band fundamental signals. The open circle denotes IM3 at 1930 MHz caused by out-band fundamental signals.

45 dBm. Another intercept point of IM3 caused by two out-band fundamental signals, which were 1945 and 1960 MHz, was at around 60 dBm. Although distortion for the 32-pole filter has not been measured, it is expected that the 32-pole filter will show almost the same-order IM3 as the result of the 16-pole filter because these two filters were designed to have almost the same bandwidth.

IV. FILTER TUNING

Filter tuning presented in this paper is based on the measurement of three fundamental design parameters of a filter: resonant frequencies of resonators, coupling coefficients between the resonators, and loaded-Q between the terminal resonators and external load. These have been measured by a novel method, which does not cause damage to the filter, such as cutting its substrate.

The tuning procedure is as follows. First, every resonant frequency of resonators that compose the filter is measured. From these results, we can identify which resonators should be tuned and how much frequency should be shifted. Second, a dielectric film is deposited on the resonators to shift resonant frequency to the desired values. In principle, a dielectric film is unable to shift resonant frequency up so resonant frequencies should be designed to be initially higher than their desired values. The shifts are adjusted through the thickness of and area covered by the dielectric film on each resonator. The purpose of this step in the tuning process is to equalize passband ripple. Therefore, after

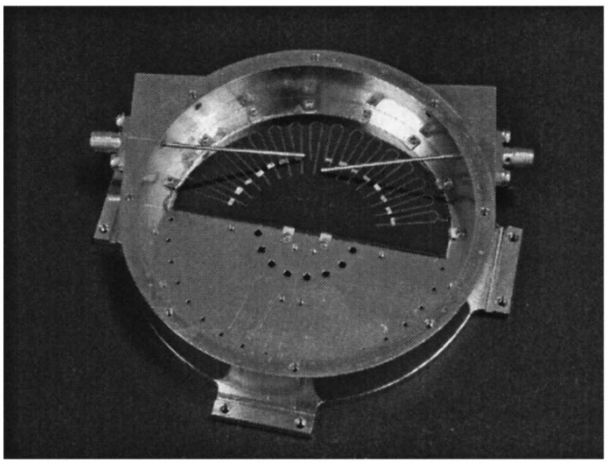

Fig. 7. Layout of resonant frequency measurement, except for the two-terminal resonators. Pieces of strip conductive tape were put on all resonators, except for the measured resonator.

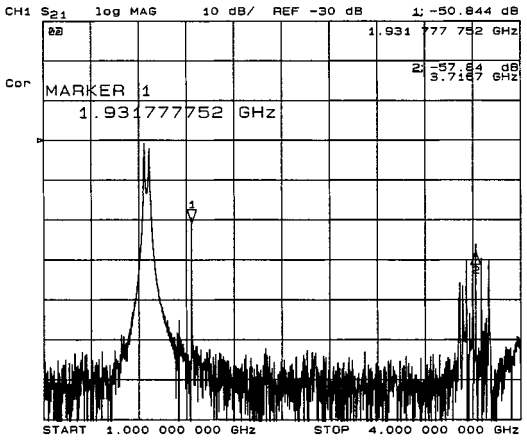

Fig. 8. Measured result of resonant frequency. The resonant frequency is indicated by MARKER 1. One of doubly shifted resonant peaks of the other resonators is indicated by MARKER 2.

this step, passband ripple is tuned but tuning of center frequency is not yet completed. Finally, a dielectric film is deposited uniformly over the entire surface of the filter. The center frequency is shifted to the proper position without the degradation of pass band ripple.

A. Method of Measurement

The idea of the method of resonant frequency measurement is simple. Two semirigid probes, which were connected with a network analyzer, were set beside each end of a resonator of which the resonant frequency was to be measured. This is similar to the well-known method of resonant frequency measurement of a single resonator. In this case, however, the other resonators affect the measurement because they have almost the same resonant frequencies and couple with the measured resonator. The interference of the other resonators must be avoided in the measurement. For that purpose, we developed the following technique. Pieces of strip conductive tape were put on the gaps between the two lines of the other J-shaped resonators to form them into closed-loop resonators. A photograph of the layout is shown in Fig. 7. By this technique, resonant frequencies of closed-loop resonators doubled because they resonated as one-wavelength resonators, while the target resonator remained a half-wavelength resonator. As a result, interference of the other resonators was removed, as shown in Fig. 8. The resonant frequency of the target resonator was measured at 1931.778 MHz (MARKER 1). Doubly shifted resonant frequencies of the reset resonators were measured at around 3.7 GHz (MARKER 2). Double peaks at around 1.7 GHz appeared as cavity modes of the instrument shown in Fig. 7. These peaks also appeared at 300 K where superconducting resonators were not able to resonate. By changing the resonators to be measured one after the other, the resonant frequency of every resonator is obtained, except for the two input and output terminal resonators. Example of measured resonant frequencies is shown in Fig. 9.

Resonant frequencies for the two-terminal resonators were measured by connecting one of two ports of the network analyzer to a probe and the other port to a filter connector. The probe

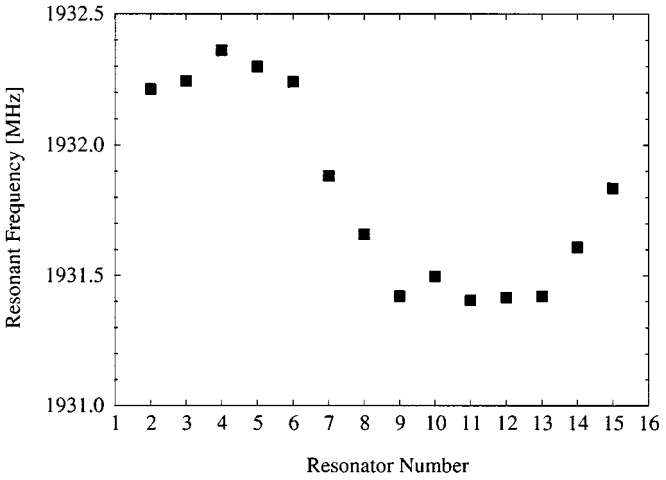

Fig. 9. Example of measured result of resonant frequencies for a 16-pole filter.

was set beside one end of the resonator. The filter connector was connected to the feed line that was tapped onto the terminal resonator. A photograph of the layout is shown in Fig. 10. Loaded-Q of the terminal resonators also can be measured by this measurement and is calculated from

$$Q_L = \frac{f_o}{\Delta}$$

where f_0 is the resonant frequency and Δ is the bandwidth at 3 dB attenuated from the top.

Coupling coefficients between two resonators can be measured in a similar way as the resonant frequency measurement. Pieces of strip conductive tape were put on all resonators, except the two coupling resonators of which the coupling coefficient was measured. Two semirigid probes were set beside each end of the two resonators. Original resonance of two resonators is split into two peaks by the effect of coupling between them, as shown in Fig. 11. The coupling coefficient k is calculated from the measured two values of peaks f_1 and f_2 as

$$k = \frac{|f_1 - f_2|}{(f_1 + f_2)/2}.$$

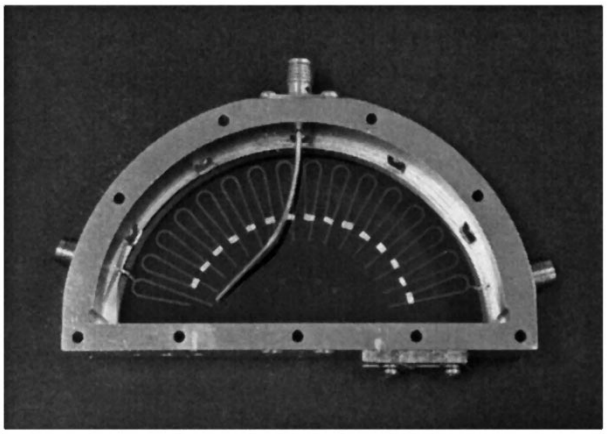

Fig. 10. Layout of resonant frequency measurement for the two-terminal resonators. Pieces of strip conductive tape were put on all resonators, except for the measured resonator.

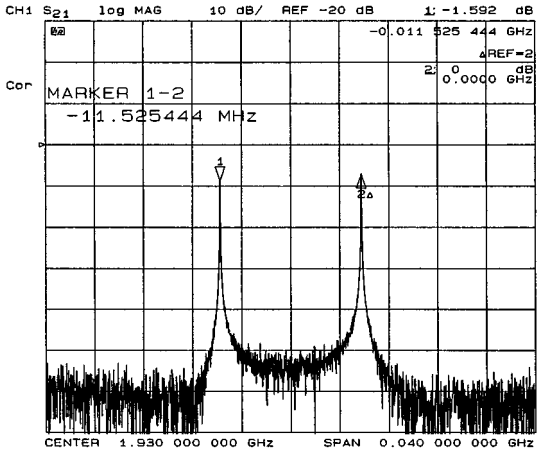

Fig. 11. Measured result of coupling resonators. Original resonance of two resonators is split into two peaks, f_1 and f_2 by the effect of coupling between them.

Both loaded-Q and coupling coefficient can be measured, but cannot be adjusted after fabrication. Therefore, the measurement should be carried out on an experimental stage before the final fabrication in order to examine the difference between EM simulation and real devices. Fig. 12 shows the results of the difference between EM simulation and measurement. Once the difference has been determined, the results are introduced in the next design process toward final fabrication. Consequently, the filters need no tuning regarding loaded-Q and coupling coefficient.

B. Method of Resonant Frequency Shift

In this paper, every resonator was tuned such that the resonant frequency was shifted to be equal to the lowest one among all resonators. To carry out deposition processes of dielectric film simultaneously for all resonators, the differences in the required shifts were converted to the deposition area of the film and its position on each resonator. The differences were digitized into 20 for convenience with satisfactory accuracy. The contribution of deposited position to the frequency shift at the end of a resonator is more effective than that at the center because the electric property is capacitive there. By taking account

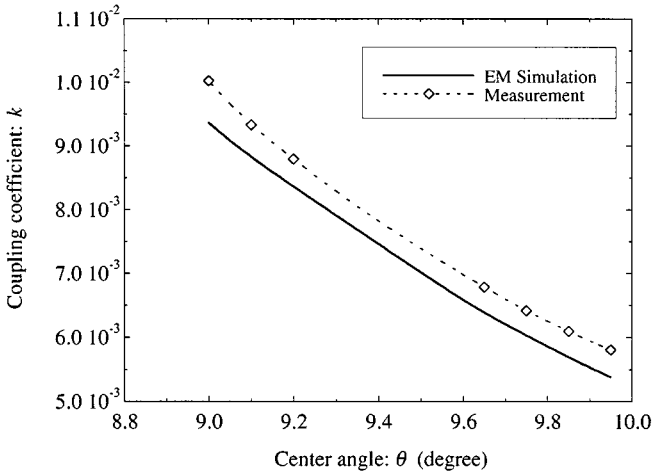

Fig. 12. Difference between the calculated and measured results of coupling coefficient.

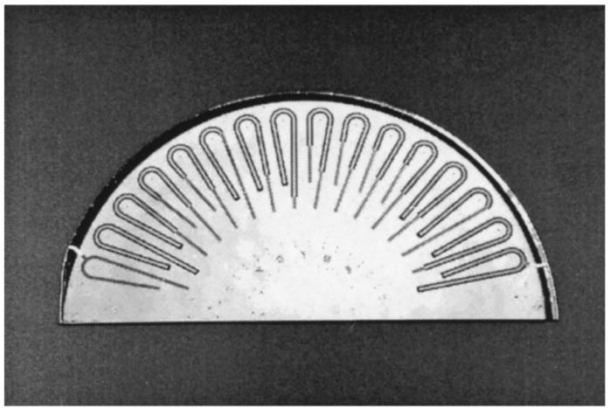

Fig. 13. Tuned 16-pole filter substrate. CeO_2 film was deposited on resonators. Deposition area and its position were different for each resonator.

of this, 20 types of photomasks were prepared corresponding to the 20 digitized differences. Dielectric film was deposited by the liftoff technique on the substrate patterned by the photomasks. Fig. 13 shows an example of a tuned 16-pole filter substrate.

As the dielectric film material, CeO_2 was used for the following reasons.

1) It is well matched with the YBCO film and MgO substrate since it is used as the buffer layer for YBCO film deposition.
2) Stable deposition is easy because it is composed of only two chemical elements.
3) It has a relatively high dielectric constant of about 26 so that it easily shifts resonant frequency.

V. Conclusion

Several lumped-element planar HTS filters have been reported [4], [5]. They have realized steep skirt band-edge slope as a result of achieving transmission zeros. The zeros were created and controlled by some cross couplings. In this paper, we approached this subject by adopting a distributed element structure. The J-shaped hairpin resonator was introduced to effectively create the transmission zeros. We selected the distributed element structure because it had the advantages of

lower insertion loss and lower IM3 over the lumped-element structure. In general, a distributed element structure has a higher Q factor and higher power-handling capability than a lumped-element structure because of the difference between their linewidths.

A novel method of filter tuning has been presented. A conventional mechanical screw is difficult to tune if filters consist of many resonators, such as the 16- or 32-pole filters. We believe that the method of measurement and tuning presented in this paper will be applicable to lumped-element filters or planar filters with more complicated layouts. This method also contributes to miniaturization of the filter's package by removing the need for tuning screws, and to high reliability owing to permanent tuning.

ACKNOWLEDGMENT

The authors would like to thank M. Okazaki, Cryodevice Inc., Yokohama, Japan, N. Tokuchi, Cryodevice Inc., Yokohama, Japan, T. Yamada, Cryodevice Inc., Yokohama, Japan, and K. Saitoh, Cryodevice Inc., Nisshin, Japan, for their helpful discussions, and Y. Nakae, DENSO Corporation, Nisshin, Japan, and T. Kamiya, DENSO Corporation, Nisshin, Japan, for filter processing.

REFERENCES

[1] G. Tsuzuki, M. Suzuki, N. Sakakibara, and Y. Ueno, "Novel superconducting ring filter," in *IEEE MTT-S Int. Microwave Symp. Dig.*, Baltimore, MD, June 1998, paper TU5E, pp. 379–382.

[2] R. Levy, "Direct synthesis of cascaded quadruplet (CQ) filters," *IEEE Trans. Microwave Theory Tech.*, vol. 43, pp. 2940–2945, Dec. 1995.

[3] J.-F. Liang and W. D. Blair, "High-Q $\mathrm{TE}_0$1 mode DR filters for PCS wireless base stations," *IEEE Trans. Microwave Theory Tech.*, vol. 46, pp. 2493–2500, Dec. 1998.

[4] J.-F. Liang, C.-F. Shih, Q. Huang, D. Zhang, and G.-C. Liang, "HTS microstrip filters with multiple symmetric and asymmetric prescribed transmission zeros," in *IEEE MTT-S Int. Microwave Symp. Dig.* , Anaheim, CA, June 1999, paper TH2D, pp. 1551–1554.

[5] G. L. Hey-Shipton, "Efficient computer design of compact planar band-pass filters using electrically short multiple coupled lines," in *IEEE MTT-S Int. Microwave Symp. Dig.* , Anaheim, CA, June 1999, paper TH2D, pp. 1547–1550.

[6] G. L. Matthaei, L. Young, and E. M. T. Jones, *Microwave Filters, Impedance-Matching Networks, and Coupling Structures*. Norwood, MA: Artech House, 1987.

Genichi Tsuzuki (M'95) received the B.Sc., M.Sc., and Ph.D. degrees in theoretical physics from Kanazawa University, Kanazawa, Japan, in 1987, 1989, and 1992, respectively, during which time he studied low-dimensional solid-state physics typified by HTS and authored several papers in this area.

In 1992, he joined the DENSO Corporation, where he was in charge of development of semiconductor devices. From 1994 to 1999, he was with Advanced Mobile Telecommunication Technology Inc. (AMTEL), where he was a Technical Staff Member. During these years, he designed and developed several HTS filters for wireless application. In 1999, he joined Cryodevice Inc., Aichi, Japan, where he is currently in charge of development of HTS filter subsystems for wireless base-stations as a Leader of the Filter Engineering Group. His current interests are accurate modeling and optimization in circuit design of microwave devices, and the application of HTS technology to high-power transmit filters.

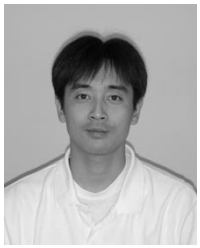

Masanobu Suzuki received the B.E. degree from Yokohama National University, Yokohama, Japan, in 1990, and the M.E. degree from Nagoya University, Nagoya, Japan, in 1992.

In 1992, he joined the DENSO Corporation, where he was engaged in research on superconducting devices. From 1994 to 1999, he was engaged in research HTS filters at Advanced Mobile Telecommunication Technology Inc. Since 1999, he has been with Cryodevice Inc., Aichi, Japan.

Nobuyoshi Sakakibara received the B.E. and M.E. degrees from Nagoya University, Nagoya, Japan, in 1979 and 1981, respectively, and the Dr. Eng. degree from the Nagoya Institute of Technology, Nagoya, Japan, in 1994.

In 1981, he joined the DENSO Corporation, where he was engaged in researches on electronic devices. From 1994 to 1999, he was engaged in researches on HTS filters at Advanced Mobile Telecommunication Technology Inc. Since 1999, he has been with Cryodevice Inc., Aichi, Japan, where he is a Section Head.